Newly Designed Tensile Test System for in vitro Measurement of Mechanical Properties of Cytoskeletal Filaments*

Shinji DEGUCHI**,***, Toshiro OHASHI** and Masaaki SATO**

A tensile test system for isolated cytoskeletal filaments, which enables to control strain rate, was newly designed. A pair of piezo-driven cantilevers were used to manipulate the specimen and to measure tensile load from the deflection of one of the cantilevers. The displacements of the cantilevers were optically and electrically detected. The specimen strain, determined from the cantilever displacements, was used as a feedback signal. We proposed a servo-system for strain rate control in which a desired path for the strain transition was designated. The path was chosen as a triangular-shape waveform against time, along which the strain rate is kept constant. We measured tensile properties of a single stress fiber isolated from a smooth muscle cell with this system to obtain a stretching stiffness of 45 nN per strain. Performance evaluation and the tensile test demonstrated that the system enabled to carry out strain rate-controlled tensile test.

Key Words: Biomechanics, Tensile Tester, Micro/Nano Manipulation, Measurement and Control, Mechanical Properties, Stress Fiber

1. Introduction

Mechanical properties of cytoskeletal filaments such as actin filaments are essential to understand intracellular stress distribution and mechanotransduction mechanism in adherent cells[1]. So far, micro/nanomanipulation techniques have been developed to evaluate mechanical properties of cytoskeletal filaments in vitro[2]-[11]. For example, optical tweezers, introduced by Ashkin[2], enabled trapping and manipulation of biological specimens by laser radiation pressure. This technique is suitable for physical manipulation of cytoskeletal filaments with high precision[3], however, the constraint of its low trapping stiffness restricts the maximum generative force to piconewton order. Cantilevers of atomic force microscope or a pair of microneedles have also been used to manipulate biological specimens and to measure the stiffness by detecting the deflection, which is proportional to loadings[4]-[11]. In contrast to the narrow measurement range of the optical tweezers, appropriate design of the microneedle shape enables force measurement with a wide force range from subpiconewton[6],[8] to micronewton[9],[10]; therefore, the microneedle technique can be more applicable to a variety of mechanical tests of biological specimen.

The microneedle technique has been developed with a combination of optical and/or electrical measurement techniques to evaluate detailed mechanical properties of biological specimens with high spatial and temporal measurement accuracy. For example, Kojima et al.[7] detected deflection of cantilever with an optical technique to study tensile properties of single actin filaments in vitro. Liu and Pollack[11] performed cyclic stretch test for single actin filaments in a wide strain range by using a photodiode array. Yasuda et al.[10] measured contraction force of single myocyte under isometric conditions with a feedback control system. Miyazaki et al.[9] obtained tensile forces in single fibroblasts from the outputs of strain gauge attached to a cantilever. These techniques contributed to better understandings of cellular or subcellular mechanics, however, no studies of tensile tester in which strain rate was arbitrarily controlled has appeared. The relationship between force and displacement of living tissues is partly affected by strain rate in mechanical test[12], and therefore the apparatus is expected to have strain rate control capability.

Here, we developed a novel tensile tester for cy-

* Received 30th May, 2005 (No. 05-4051)

** Department of Bioengineering and Robotics, Graduate School of Engineering, Tohoku University, 6–6–01 Aobayama, Sendai 980–8579, Japan

*** Department of Energy Systems Engineering, Graduate School of Natural Science and Technology, Okayama University, 3–1–1 Tsushima-naka, Okayama 700–8530, Japan. E-mail: deguchi@mech.okayama-u.ac.jp

toskeletal filaments with the capability to control strain rate. A pair of cantilevers was used to stretch specimen. Both of deflection of the cantilever, which was proportional to tensile loading, and strain of the specimen were detected with optical and electrical ways. We demonstrated that moving velocity of the cantilever was controlled by a servo control system. We finally showed an application example of the tensile tester in which force–strain relation of a single stress fiber (bundled actin cytoskeletal filament[1]) was examined at a constant strain rate.

2. Development of Tensile Test System

2.1 Actuator

A tensile tester was built on an inverted fluorescence microscope (IX-71, Olympus, Tokyo, Japan) (Fig. 1). The microscope was fixed on a vibration-free table in a dark room. A glass rod (1 mm in diameter) was drawn with a glass-electrode puller (PP-83, Narishige, Tokyo, Japan) to have a tip of an ~20-μm diameter. A carbon fiber (Toray, Tokyo, Japan), 7 μm in diameter, was attached to the tip of the rigid glass rod with epoxy adhesive. This carbon fiber increases optical contrast and then facilitates optical measurements of its displacement. The carbon fiber–glass rod structure, referred to as cantilever, was used to manipulate a specimen. A pair of cantilevers (deflectable and non-deflectable cantilevers) was used to stretch the specimen. The length of the carbon fiber part of the deflectable cantilever was set ~300–800 μm. The stiffness for deflection of the deflectable cantilever was determined by cross-calibration against a glass needle with a known spring constant[5] to be 0.001 1–0.046 N/m. The length of the carbon fiber part of the non-deflectable cantilever was set ~50 μm. The tips of the cantilevers were immersed in PBS in a culture dish placed on the microscope stage. The positions of cantilevers were adjusted by using hydraulic micromanipulators (MMO-203, Narishige) to bring the tips in contact with a specimen. The deflectable cantilever was placed at one end of the specimen vertically to the specimen, while the non-deflectable cantilever was placed at the other end in parallel to the specimen (Fig. 2 (a)); therefore, the latter did not bend against tensile loadings. The cantilevers were displaced by using piezoelectric ceramic actuators (PZT, AE0505D16, NEC Tokin, Sendai, Japan) connected to each base glass rod (Fig. 1) for applying tensile loadings onto the specimen. Driving voltages for the PZT was generated with a personal computer (Evo N110, Compaq, Hewlett-Packard, Palo Alto, CA) equipped with an A/D converter (DAQ Card-1200, National Instruments, Austin, TX) and amplified with a piezo driver (HPZT-0.15P, Matsusada Precision, Shiga, Japan).

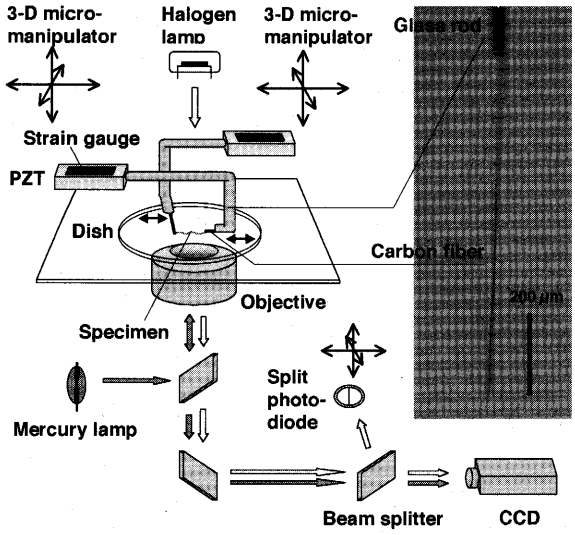

Fig. 1 Schematic diagram of the tensile tester

2.2 Sensor

The position of the tip of the deflectable cantilever was tracked with a photosensing system. The system consists of a circular split photodiode separated by a gap of 20 μm (S1557, 1.0 mm in diameter, Hamamatsu Photonics, Hamamatsu, Japan), a current–voltage (I-V) converter, and a differential amplifier (Fig. 2 (b)). A halogen lamp activated by a stabilized DC power supplier (GP035-10, Takasago, Kawasaki, Japan) was used to illuminate the cantilevers. The image of the tip of the deflectable cantilever was magnified through a 20x objective and pro-

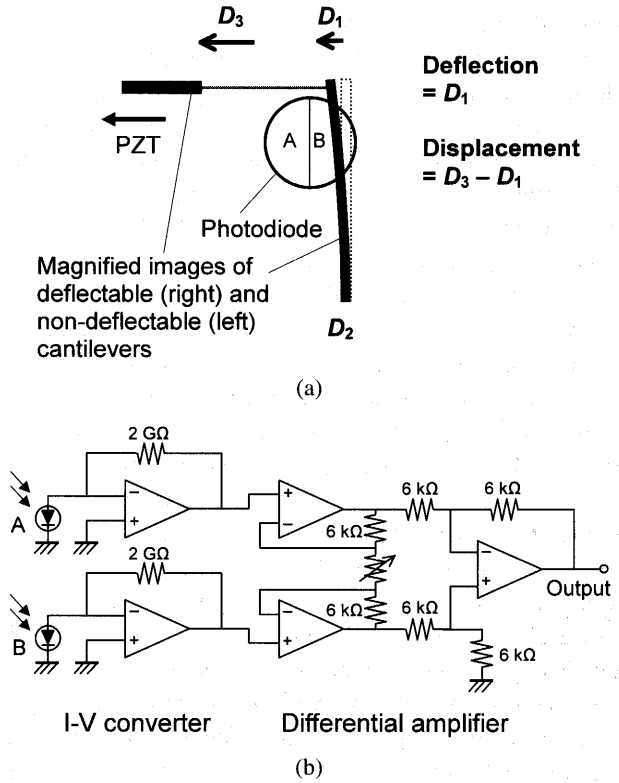

Fig. 2 Detection system of the tensile tester. (a) Schema of the tensile test. Cantilever deflection is exaggerated in this diagram. (b) Circuit diagram of the photosensing system

jected onto a custom-built beam splitter (Olympus) at the side port of the microscope (Fig. 1). The beam splitter was designed to reflect 70% of the incident light into the photodiode and to transmit the rest into a digital CCD camera (C4742-95, Hamamatsu Photonics). The position of the photodiode was adjusted by the use of a micromanipulator. The output of the photodiode was obtained through the I-V converter made of operational amplifiers (OPA111BM, Texas instruments, Dallas, TX) with feedback resistances of 2 GΩ (RH1/4HVC, Japan hydrazine, Tokyo, Japan)[13]. The difference between each output was obtained through the differential amplifiers (INA103KP, Texas instruments). The output was obtained with the A/D converter through voltage followers, non-inverting amplifiers, and quadratic low pass filters (cut-off frequency = 730 Hz).

A strain gauge system was used to measure the extension of PZTs. A strain gauge (Kyowa electronic instruments, Tokyo, Japan) was attached to the surface of the PZT. Voltages generated by the extension of the PZT were detected by a bridge circuit (NEC, Tokyo, Japan), amplified by a strain amplifier (AS1203, NEC), and recorded on the computer.

2.3 Control

In sensors calibration, the base part of the deflectable cantilever was moved by using the PZT. Output voltages of the photosensing system corresponding to the displacement of the cantilever tip (D_1 in Fig. 2 (a)) and the strain gauge system corresponding to the displacement of the cantilever base (D_2) were recorded. In tensile test, the non-deflectable cantilever was moved apart from the deflectable cantilever using the PZT to stretch a specimen. The base of the deflectable cantilever was fixed, and then $D_2 = 0$. Output voltages of the photosensing system and the strain gauge system corresponding to the displacements of the deflectable (D_1) and the non-deflectable (D_3) cantilever tips, respectively, were obtained.

In order to control strain rate, a servo control was performed as follows. Before each experiment, calibrations for both the photosensing system and the strain gauge system were carried out, providing relationships between those outputs and the displacements. A reference input, which has a triangular-shape waveform, was used for moving the cantilever as a desired displacement path along which the slope of displacement–time curve is constant; therefore, the moving velocity can be kept constant. In a strain rate feedback control, the output that corresponds to the displacement of specimen ($D_3 - D_1$) was detected, divided by the initial length to obtain the strain of the moment, and compared with a reference input having a designated triangular-shape waveform. The error signals were sent to a PID controller written in LabVIEW programming language (National Instruments) to obtain an appropriate control gain for driving the PZT.

2.4 Tensile test

To test the feasibility of strain rate control, tensile test of a single stress fiber was conducted. Stress fibers were isolated from cultured bovine aortic smooth muscle cells according to the reported technique[14], stained with rhodamine-phalloidin, and suspended in PBS in a 35-mm diameter suspension culture dish (Sumilon, Tokyo, Japan). Before experiment, epoxy glue (Araldite, Vantico, Japan) was coated on the tips of the cantilevers. Under illumination from the halogen and mercury lamps, the cantilevers successfully holding the stress fiber were held for 10 min in the solution until the glue hardened. Initial length of the stress fiber was obtained with the CCD camera. Tensile tests were initiated under halogen light illumination while controlling the non-deflectable cantilever to apply tensile loads at a 0.02-s^{-1} strain rate. Cross-calibration of the deflectable cantilever yielded the force–strain relation of the stress fiber. All experiments were performed at room temperature.

3. Results

3.1 Performance evaluation

The relation between extensions of the PZT and driving voltages was first examined. The deflectable cantilever was displaced in a step-wise manner with the PZT. Images were taken at each driving voltage. The displacement of the cantilever was measured from the images by using image analysis software (IPLab, Signal Analytics Corporation, Vienna, VA). The result showed that large hysteresis appeared, which is a common characteristic of the piezoelectric actuator with a high piezoelectric constant[15]. A serial connection of a capacitor with a low capacitance of 0.47 μF reduced the hysteresis and partly compensated for the nonlinearity of the actuator. Here, the maximum extension of the PZT with the capacitance was 6.9 μm.

To estimate the spatial and the temporal measurement accuracy of the strain gauge system and the photosensing system, a step-wise change in driving voltage was applied to the PZT, and the resultant responses of both sensors were recorded (Fig. 3). The voltage responses were converted to the displacements of cantilever using the slope of the curve obtained in the calibration for the PZT. The output sensitivities of strain gauge system and the photosensing system were determined as 1.1 mV/nm and 0.35 mV/nm, respectively. The maximum noise level was ~5 mV for the strain gauge system and ~15 mV for the photosensing system, thereby estimating the spatial measurement accuracy to be ~5 nm for the strain gauge system and ~43 nm for the photosensing system. The working range of the photosensing system in the calibration was ~12 μm. The time constants of both sensors were limited by the sampling time to 1 ms.

In a calibration for the strain gauge system, an increasing step-wise voltage (V_{I1}) was applied to the PZT

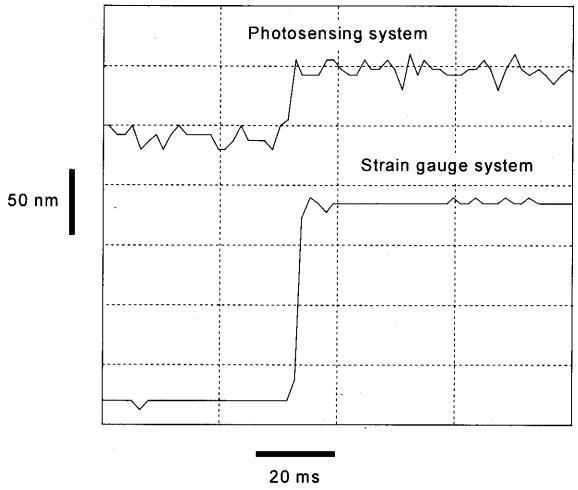

Fig. 3 Time course of the change in sensors when a sudden displacement change was applied to the cantilever. The output voltages were converted to the displacements after calibrations

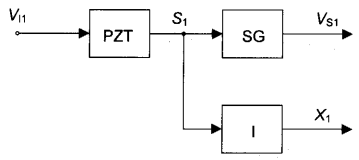

I, Image analysis software; SG, Strain gauge system; S_1, Strain of PZT; V_{I1}, Increasing step-wise input; V_{S1}, Strain gauge system output; X_1, Displacement of cantilever base.

(a)

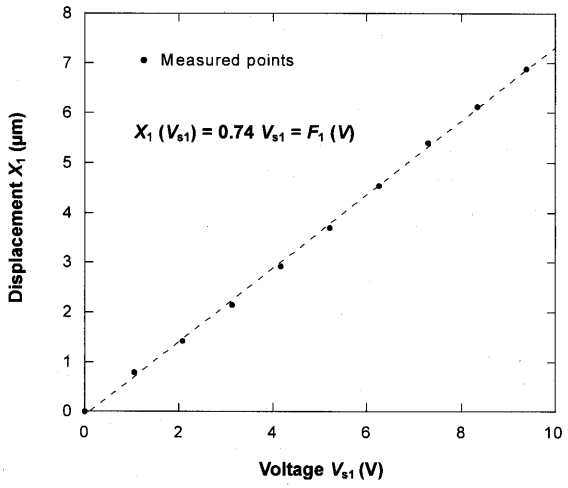

(b)

Fig. 4 Calibration of the strain gauge system. (a) Calibration procedure. (b) Relation between the displacement and the strain gauge system output. The fitting function was obtained by least-squares regression

(Fig. 4 (a)). The outputs of strain gauge (V_{S1}) were recorded, and simultaneously the images of cantilever were acquired at each step. Displacements at given voltages (X_1) were obtained using image analysis software (IPLab). In the image analysis, a single pixel corresponded to a 0.16-μm length. The slope of V_{S1}–X_1 curve, $F_1(V)$, was then obtained (Fig. 4 (b)). In the present example, $F_1(V) = 0.74V$.

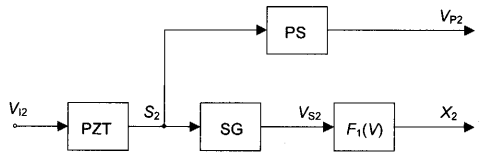

$F_1(V)$, Fitting function of strain gauge system curve; PS, Photosensing system; SG, Strain gauge system; S_2, Strain of PZT; V_{I2}, Linearly increasing input; V_{P2}, Photosensing system output; V_{S2}, Strain gauge system output; X_2, Displacement of cantilever tip.

(a)

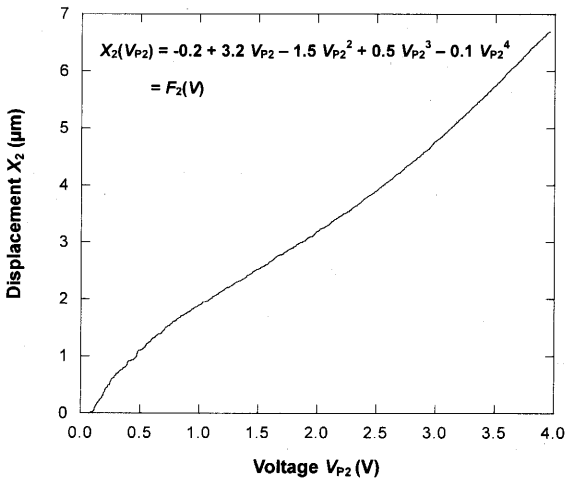

(b)

Fig. 5 Calibration of the photosensing system. (a) Calibration procedure. (b) Relation between the displacement and the photosensing system output. The fitting function was obtained by least-squares regression

In a calibration for the photosensing system, a linearly increasing voltage (V_{I2}) was applied to the PZT (Fig. 5 (a)). Outputs of the strain gauge (V_{S2}) and the photosensing system (V_{P2}) were recorded simultaneously. The displacement of the cantilever base (X_2) was calculated from $F_1(V)$. The least-squares regression for the V_{P2}–X_2 curve, $F_2(V)$, was then obtained in a quartic form (Fig. 5 (b)). In the present example, $F_2(V) = -0.2 + 3.2V - 1.5V^2 + 0.5V^3 - 0.1V^4$.

To evaluate strain rate-control performance, a servo control system shown in Fig. 6 (a) was investigated. A triangular-shape waveform (V_{I3}, amplitude = 5 μm, frequency = 0.05 Hz) was applied as a desired path along which the cantilever displacement should follow. Displacement of the tip of cantilever was detected by the photosensing system and the function $F_2(V)$. The error signal, which is the difference between the reference input and the primary feedback signal, was sent to the PID controller. The output of the strain gauge system was converted to the displacement of the cantilever base by using the func-

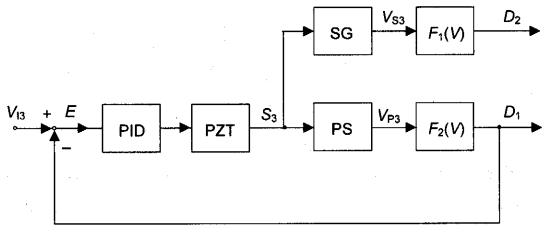

$F_1(V)$, Fitting function of strain gauge system curve; $F_2(V)$, Fitting function of photosensing system curve; PID, PID controller; PS, Photosensing system; SG, Strain gauge system; D_1, Displacement of cantilever tip; D_2, Displacement of cantilever base; E, Actuating error signal; S_3, Strain of PZT; V_{I3}, Triangular waveform input; V_{P3}, Photosensing system output; V_{S3}, Strain gauge system output.

(a)

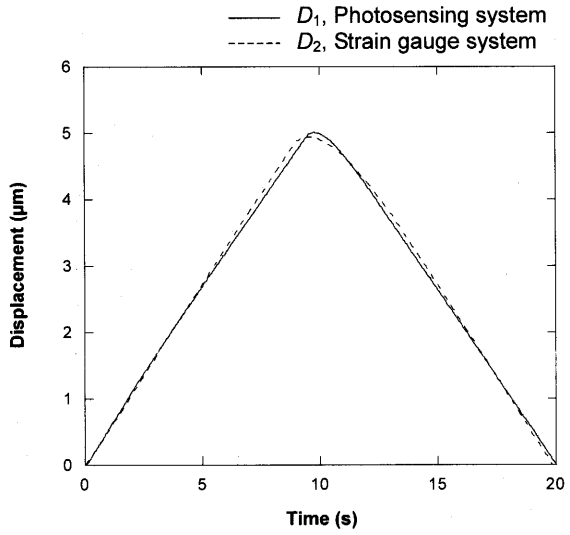

(b)

Fig. 6 Servo system for strain rate control. (a) Circuit diagram of strain rate feedback control. (b) The displacements of cantilever tip (D_1) and base (D_2) vs. time

tion $F_1(V)$. As expected, the outputs of both sensors were controlled to trace the desired triangular waveform, indicating that the tip and the base part of the cantilever were moved at a constant rate (Fig. 6 (b)).

3.2 Tensile test

A servo control system shown in Fig. 7 (a) was used for the tensile test. A triangular-shape waveform (V_{I4}, maximum strain = 0.1, strain rate = 0.02 s^{-1}) was applied as a desired path for strain trajectory. The signals that correspond to the displacement of specimen ($D_3 - D_1$) were divided by the initial length of the specimen (42.0 μm) to obtain the strain of the moment and were fed back to be compared with the reference inputs. The error signals were sent to the PID controller to obtain appropriate gain inputs for the PZT connected to the non-deflectable cantilever.

A rhodamine-labeled stress fiber was captured by the cantilevers under the mercury and halogen light illuminations (Fig. 7 (b)) and then stretched under the halogen light illumination. The force–strain relation was shown in Fig. 7 (c). Changes in the positions of cantilevers (D_1 and D_3) and resultant strain ($D_3 - D_1$ divided by the initial length) during the test were shown in Fig. 7 (d). Although each cantilever displacement and the resultant force–strain relation showed curving trajectories, the strain waveform followed the desired straight paths in the loading and unloading processes. As expected in addition, the maximum strain reached 0.1 at 5 s, indicating that the tensile test was performed at the constant rate of 0.02 s^{-1}. A hysteresis and a residual strain were observed in the force–strain curve. The stretching stiffness, defined as the slope of the least-squares regression linear function of the force–strain curve for loading process, was 45 nN per strain.

4. Discussion

The past tensile testers for micro/nano biological specimen[5),(7),(9),(11)] did not possess a functional capability to control strain rate, an important parameter for evaluation of the tensile properties. In the present study, we newly designed a tensile test system, which performs tensile test at a desired strain rate by a feedback system. In order to regulate strain rate, we detected the position of the tip of each cantilever to obtain the strain of specimen. Then, the cantilever position was servo-controlled to follow a designated path. If we chose the path as a triangular-shape waveform against time, the distance between the cantilevers, corresponding to the strain of the moment if divided by the initial length, would change at the constant rate equal to the slope of the triangular-shape waveform. In consequence, we could keep the strain rate constant while conducting tensile test (Figs. 6 (b) and 7 (b)), suggesting that the proposed servo-control system can contribute to carrying out strain rate-controlled micro tensile test.

To achieve a strain rate-controlled tensile test, accurate detection of each cantilever tip position is of importance. Here, the displacement of the non-deflectable cantilever tip (D_3) was obtained by the strain gauge system attached to the PZT. In general, PZT has hysteresis characteristics come from the intrinsic crystal structure in its applied voltage–extension curve[16)]. We connected the capacitor of low capacitance serially to reduce the nonlinear effect partly. This technique is simple and takes low cost for the linear compensation, however, it results in a decrease in the sensitivity of the PZT. In the present study, the PZT hysteresis does not actually restrict the precision of tensile test since the displacement of cantilever was determined and controlled based on outputs of the strain gauge system whose strain–output relation is linear[16)]. On the other hand, the displacement of the deflectable cantilever (D_1) was obtained by the photosensing system as calibrated in Fig. 5. To compensate for its nonlinear per-

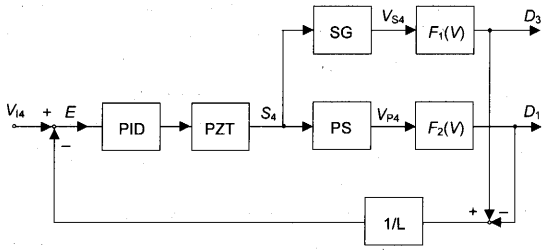

$F_1(V)$, Fitting function of strain gauge system curve; $F_2(V)$, Fitting function of photosensing system curve; PID, PID controller; PS, Photosensing system; SG, Strain gauge system; D_1, Displacement of deflectable cantilever tip; D_3, Displacement of non-deflectable cantilever tip; E, Actuating error signal; S_4, Strain of PZT; V_{I4}, Triangular waveform input; V_{P4}, Photosensing system output; V_{S4}, Strain gauge system output.

(a)

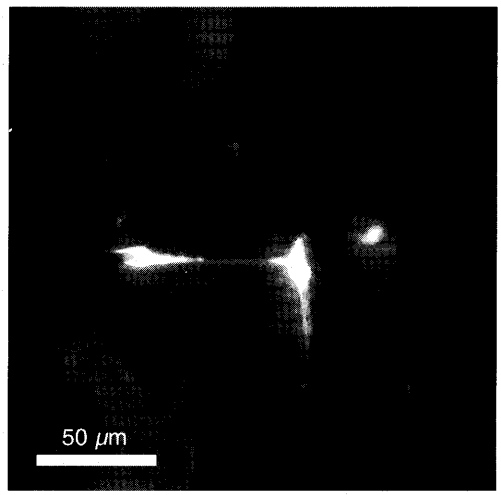

(b)

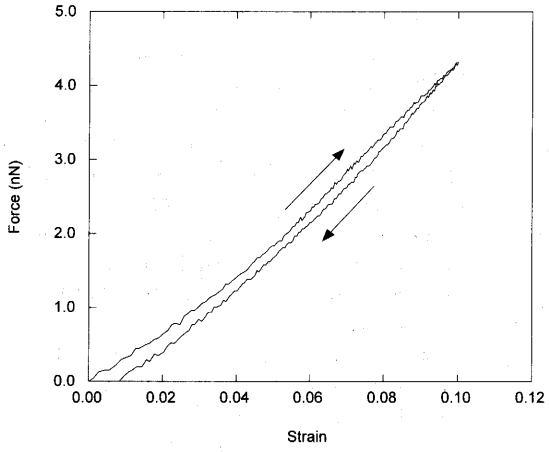

(c)

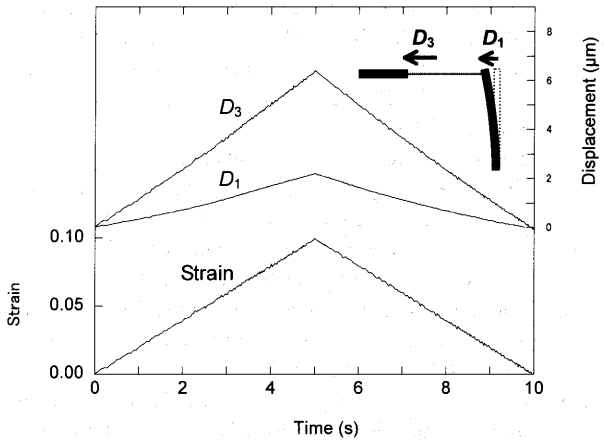

(d)

Fig. 7 Tensile test of a stress fiber. (a) Circuit diagram of the servo-control system. (b) Typical fluorescence image of the initial state of the tensile test. The stress fiber was captured by cantilevers. (c) Tensile force vs. strain. (d) Strain and displacement of deflectable (D_1) and non-deflectable (D_3) cantilever tips vs. time

formance, we linearized the response with the fitting function represented by polynomial equations such as $F_2(V)$. The base part of the deflectable cantilever was fixed, and then the deflection corresponded to the tip displacement. Strain of specimen was then obtained as $(D_3 - D_1)$/(Initial length) with high spatial and temporal measurement accuracy.

We demonstrated a tensile test of a single stress fiber to evaluate control performance of the servo-system and found that the stiffness was 45 nN per strain. If cross-sectional area of the stress fiber is calculated assuming that it was a continuum material and its cross-section was the circle with a 100-nm radius based on our preliminary electron microscopy, then the Young's modulus is 1.4 MPa. In contrast, it was reported that the Young's modulus of actin filaments, a major component of stress fiber, was 1.8 GPa[7]. Since stress fibers are composed of bundled actin filaments with associated proteins such as myosin and α-actinin[14], the structural difference might be responsible for the difference in the Young's modulus. Characterization of detailed mechanical properties of stress fibers will be the subject of future investigation. The stress fiber plays an important role in bearing intracellular stresses; therefore, knowledge of the mechanical properties will be crucial for considering its role in mechanotransduction[1]. The system developed here can contribute to better understandings of the mechanical properties of such biological specimens.

5. Conclusions

We newly designed a tensile test system for isolated cytoskeletal filaments with strain rate control capability. In the system, we proposed a servo-system for strain rate control in which a desired path for the strain transition was designated. We measured stretching stiffness of a single stress fiber isolated from a smooth muscle cell with this system while keeping the strain rate constant. Performance evaluation and the tensile test demonstrated that the

system enables to carry out strain rate-controlled tensile test and is useful for studies of cytoskeletal mechanics.

Acknowledgements

This work was supported in part by the Grants-in Aids for Scientific Research (A) (No. 14208100) and for Explorary Research (No. 17650125), 21st Century Program 'Future Medical Engineering Based on Bio-nanotechnology' granted to the Tohoku University by the Ministry of Education, Culture, Sports, Science and Technology in Japan, and the Sasakawa Scientific Research Grant from Japan Science Society.

References

(1) Davies, P.F., Zilberberg, J. and Helmke, B.P., Spatial Microstimuli in Endothelial Mechanosignaling, Circ. Res., Vol.92 (2003), pp.359–370.

(2) Ashkin, A., Dziedzic, J.M., Bjorkholm, J.E. and Chu, S., Observation of a Single-Beam Gradient Force Optical Trap for Dielectric Particles, Opt. Lett., Vol.11 (1986), pp.288–290.

(3) Ishijima, A., Kojima, H., Funatsu, T., Tokunaga, M., Higuchi, H., Tanaka, H. and Yanagida, T., Simultaneous Observation of Individual ATPase and Mechanical Events by a Single Myosin Molecule during Interaction with Actin, Cell, Vol.92 (1998), pp.161–171.

(4) Kamimura, S. and Takahashi, K., Direct Measurement of the Force of Microtubule Sliding in Flagella, Nature, Vol.293 (1981), pp.566–568.

(5) Kishino, A. and Yanagida, T., Force Measurements by Micromanipulation of a Single Actin Filament by Glass Needles, Nature, Vol.334 (1988), pp.74–76.

(6) Ishijima, A., Doi, T., Sakurada, K. and Yanagida, T., Sub-Piconewton Force Fluctuations of Actomyosin in Vitro, Nature, Vol.352 (1991), pp.301–306.

(7) Kojima, H., Ishijima, A. and Yanagida, T., Direct Measurement of Stiffness of Single Actin Filaments with and without Tropomyosin by in Vitro Nanomanipulation, Proc. Natl. Acad. Sci. USA, Vol.91 (1994), pp.12962–12966.

(8) Tokunaga, M., Aoki, T., Hiroshima, M., Kitamura, K. and Yanagida, T., Subpiconewton Intermolecular Force Microscopy, Biochem. Biophys. Res. Commun., Vol.231 (1997), pp.566–569.

(9) Miyazaki, H., Hasegawa, Y. and Hayashi, K., A Newly Designed Tensile Tester for Cells and Its Application to Fibroblasts, J. Biomech., Vol.33 (2000), pp.97–104.

(10) Yasuda, S., Sugiura, S., Kobayakawa, N., Fujita, H., Yamashita, H., Katoh, K., Saeki, Y., Kaneko, H., Suda, Y., Nagai, R. and Sugi, H., A Novel Method to Study Contraction Characteristics of a Single Cardiac Myocyte Using Carbon Fibers, Am. J. Physiol. Heart. Circ. Physiol., Vol.281 (2001), pp.H1442–H1446.

(11) Liu, X. and Pollack, G.H., Mechanics of F-Actin Characterized with Microfabricated Cantilevers, Biophys. J., Vol.83 (2002), pp.2705–2715.

(12) Fung, Y.C., Biomechanics, Mechanical Properties of Living Tissues, Second Edition, (1993), pp.34–35, Springer-Verlag.

(13) Kamimura, S., Direct Measurement of Nanometric Displacement under an Optical Microscope, Appl. Optics, Vol.26 (1987), pp.3425–3427.

(14) Katoh, K., Kano, Y., Masuda, M., Onishi, H. and Fujiwara, K., Isolation and Contraction of the Stress Fiber, Mol. Biol. Cell, Vol.9 (1998), pp.1919–1938.

(15) Kaizuka, H. and Siu, B., A Simple Way to Reduce Hysteresis and Creep When Using Piezoelectric Actuators, Jpn. J. Appl. Phys., (in Japanese), Vol.27 (1988), pp.773–776.

(16) Jiang, Z., Chonan, S., Yamamoto, T. and Fuda, Y., Linear Compensation of Piezoactuator's Hysteresis (1st Report, Strain Feedback and Self-Sensing Control Methods), Trans. Jpn. Soc. Mech. Eng., (in Japanese), Vol.64, No.617, C (1998), pp.149–155.